The ISME Journal (2014) 8, 2453–2462

www.nature.com/ismej

ORIGINAL ARTICLE

Magnetosome-containing bacteria living as symbionts of bivalves

Suzanne C Dufour[1], Jason R Laurich[1], Rebecca T Batstone[1,3], Bonita McCuaig[1], Alexander Elliott[1,4] and Kristin M Poduska[2]

[1]*Department of Biology, Memorial University of Newfoundland, St John's, Newfoundland A1B 3X9, Canada and* [2]*Department of Physics and Physical Oceanography, Memorial University of Newfoundland, St John's, Newfoundland A1B 3X7, Canada*

Bacteria containing magnetosomes (protein-bound nanoparticles of magnetite or greigite) are common to many sedimentary habitats, but have never been found before to live within another organism. Here, we show that octahedral inclusions in the extracellular symbionts of the marine bivalve *Thyasira* cf. *gouldi* contain iron, can exhibit magnetic contrast and are most likely magnetosomes. Based on 16S rRNA sequence analysis, *T.* cf. *gouldi* symbionts group with symbiotic and free-living sulfur-oxidizing, chemolithoautotrophic gammaproteobacteria, including the symbionts of other thyasirids. *T.* cf. *gouldi* symbionts occur both among the microvilli of gill epithelial cells and in sediments surrounding the bivalves, and are therefore facultative. We propose that free-living *T.* cf. *gouldi* symbionts use magnetotaxis as a means of locating the oxic–anoxic interface, an optimal microhabitat for chemolithoautotrophy. *T.* cf. *gouldi* could acquire their symbionts from near-burrow sediments (where oxic–anoxic interfaces likely develop due to the host's bioirrigating behavior) using their superextensile feet, which could transfer symbionts to gill surfaces upon retraction into the mantle cavity. Once associated with their host, however, symbionts need not maintain structures for magnetotaxis as the host makes oxygen and reduced sulfur available via bioirrigation and sulfur-mining behaviors. Indeed, we show that within the host, symbionts lose the integrity of their magnetosome chain (and possibly their flagellum). Symbionts are eventually endocytosed and digested in host epithelial cells, and magnetosomes accumulate in host cytoplasm. Both host and symbiont behaviors appear important to symbiosis establishment in thyasirids.

The ISME Journal (2014) **8,** 2453–2462; doi:10.1038/ismej.2014.93; published online 10 June 2014

Introduction

A taxonomically and ecologically diverse group of free-living bacteria are magnetotactic: their cytoplasm contains one or more chains of protein-bound, biomineralized magnetite or greigite ('magnetosomes'), producing a magnetic dipole within the cell (Lefèvre and Bazylinski, 2013). Magnetotactic bacteria can align with the Earth's magnetic field and move along geomagnetic field lines using their flagella. Many magnetotactic bacteria are chemolithoautotrophic microaerophiles that use magnetotaxis to locate the oxic–anoxic interface (OAI) within sediments, a favorable environment for them due to the proximity of reduced compounds (for example, hydrogen sulfide) and oxygen (Lefèvre and Bazylinski, 2013).

Although most chemolithoautotrophic bacteria have a free-living existence, some form obligate or facultative symbioses with marine invertebrates (Dubilier *et al.*, 2008). The sulfur-oxidizing symbionts of thyasirid bivalves are among the few examples of chemosymbionts that are likely facultative (that is, capable of living both in hosts and in the outside environment), given that they are located outside rather than inside host gill cells (Southward, 1986; Dufour, 2005) and that, in at least one species (*Thyasira* n. sp. Guiness), host individuals can associate with different symbiont phylotypes, suggesting acquisition from surrounding sediments (Duperron *et al.*, 2012a). Nevertheless, bacteria that associate with thyasirids are considered to be symbionts and not merely microbes trapped on gill epithelia as water circulates within the pallial cavity, because individual hosts associate with a single dominant phylotype of sulfur-oxidizing bacteria (Duperron *et al.*, 2012b). Intriguingly, transmission electron micrographs of the gills of at

Correspondence: SC Dufour, Department of Biology, Memorial University of Newfoundland, 232 Elizabeth St, St John's, Newfoundland A1B 3X9, Canada.
E-mail: sdufour@mun.ca
[3]Current address: Department of Ecology and Evolutionary Biology, University of Toronto, Toronto, Ontario, Canada M5S 3G5.
[4]Current address: Department of Biological Sciences, University of Calgary, Calgary, Alberta, Canada T2N 1N4.
Received 20 February 2014; revised 6 May 2014; accepted 8 May 2014; published online 10 June 2014

least four thyasirid species reveal that their symbionts contain abundant electron-dense inclusions, interpreted as being viruses (Southward and Southward, 1991; Brissac *et al.*, 2011; Duperron *et al.*, 2012b).

Thyasira cf. *gouldi* from Bonne Bay were recently described as forming a cryptic complex in which there are two symbiotic operational taxonomic units (OTUs 1 and 2) and an asymbiotic OTU (3) of bivalves, which vary slightly in shell shape (Batstone *et al.*, 2014). Similar to other thyasirids (Southward, 1986; Dufour, 2005), the symbionts of *T.* cf. *gouldi* OTUs 1 and 2 are maintained at the surface of gill epithelial cells within extracellular 'pockets' bounded by cytoplasmic extensions of host cells that often bear microvilli (Batstone *et al.*, 2014). Symbiotic thyasirids meet part of their nutritional requirements by assimilating carbon fixed by symbionts (Dando and Spiro, 1993), and electron micrographs show that symbionts are periodically engulfed within gill epithelial cells, a process that results in whorls of lysed bacterial products in host cells (Southward, 1986; Dufour, 2005). As thyasirid symbionts are held among gill epithelial cells, they likely benefit from host bioirrigation and sulfur-mining behaviors, which give them access to oxygen and reduced sulfur (Dufour and Felbeck, 2003; Dando *et al.*, 2004).

Here, we use multiple lines of evidence to show that inclusions in the symbionts of *Thyasira* cf. *gouldi* from Bonne Bay, Canada contain iron (most likely iron sulfide), can show magnetic contrast and, in some cases, are arranged in distinct chains; this is the first report of invertebrates forming associations with bacteria that contain magnetosomes.

Materials and methods

Sample collection and dissection

Sediments were collected from three sites (Deer Arm: 30 m depth; Southeast Arm: 30 m depth; and Neddy's Harbour: 15 m depth) in the fjord of Bonne Bay, Newfoundland, Canada, during multiple collection trips between September 2009 and November 2013. Sediments were sieved on a 1 mm mesh and symbiotic individuals of *Thyasira* cf. *gouldi* were retained; symbiotic and asymbiotic *T.* cf. *gouldi* were sorted on the basis of shell shape and gill morphology upon dissection (Batstone *et al.*, 2014). We could not distinguish between the two symbiotic OTUs (which differ in 18S, 28S and CO1 gene sequences but not in morphological characters), so all specimens analyzed herein consist of either OTU 1 (the most common type) or OTU 2.

Upon dissection, the color of the gills (which varied from pale-pink to black) was noted. Gills of dissected individuals underwent different treatments: some were rinsed in distilled water and individually placed in vials of 95% ethanol for DNA extraction and analysis (see below), while others were fixed in 2.5% glutaraldehyde in 0.1 M sodium cacodylate buffer (24 h) for either transmission electron microscopy (TEM), selected area electron diffraction (SAED), histological staining or environmental scanning electron microscopy (ESEM) and elemental analysis. Symbionts from the gill of one individual were isolated immediately for atomic force microscopy/magnetic force microscopy (AFM/MFM), as described below.

TEM

To observe symbionts, gills were post-fixed in 1% osmium tetroxide in 0.1 M sodium cacodylate buffer (1 h), dehydrated in an ascending ethanol series and embedded in TAAB 812 resin (Canemco, Canton de Gore, QC, Canada). Ultra-thin (60 nm) transverse gill sections were post-stained with uranyl acetate and lead citrate, and imaged using a Philips 300 transmission electron microscope (Tokyo, Japan).

Histological staining for iron

A prussian blue histological staining protocol (Sheehan and Hrapchak, 1980) was used to localize iron in the gills of 11 *Thyasira* cf. *gouldi* specimens. Gills were dehydrated in an ascending ethanol series (without post-fixation in osmium), embedded in paraffin and sectioned (5 μm thick). Deparaffinized and hydrated transverse sections of gill filaments were immersed for 20 min in a freshly prepared solution of 10% aqueous hydrochloric acid and 5% aqueous potassium ferrocyanide, rinsed three times in distilled water and counterstained with Hematoxylin (1 min) before dehydration, cover slipping and imaging with a Zeiss light microscope (Munich, Germany).

Elemental analysis

To investigate whether symbiont inclusions contained iron, we mounted thin (1 μm) resin sections of one gill (post-fixed in 1% osmium tetroxide) on stubs for ESEM and elemental analysis. We used a standard (solid state) backscattered electron detector in an FEI Quanta 650F ESEM (Eindhoven, The Netherlands) to observe and image symbiont inclusions in combination with a Bruker XFlash SSD 5030 X-ray detector (Berlin, Germany) for elemental analysis.

AFM/MFM

We used AFM/MFM to determine whether inclusions are magnetic, as in (Proksch *et al.,* 1995). Symbionts were isolated from a single gill using a Percoll cushion (Distel and Felbeck, 1988), smeared on a glass slide, air-dried and magnetized by placing a magnet perpendicular to the plane of the slide for tens of seconds. We used an Asylum Research MFP-3D Atomic Force Microscope (Santa Barbara, CA, USA), operating in an interleaved AC/lift mode, for

all imaging. A Co-Cr coated tip (Mikromasch NSC36, Wetzlar, Germany) was magnetized perpendicular to the cantilever plane before imaging, and samples were magnetized in the plane of the slide. Lift heights of 35–150 nm were tested for magnetic contrast imaging.

SAED

The crystal structure of inclusions was studied using SAED. Resin-embedded gill sections were coated with carbon and then examined in a FEI Titan low base TEM (Eindhoven, The Netherlands) operated at 300 kV. Electron diffraction patterns were obtained by focusing the beam on either one or two inclusions at a time, and d-spacings were determined from these patterns.

DNA extraction and amplification

To identify symbionts, DNA was extracted from the gills of three *Thyasira* cf. *gouldi* specimens (following confirmation of symbiont inclusions in the other gill using TEM) using the QIAgen DNeasy Blood and Tissue kit (Hilden, Germany), following the spin-column protocol for animal tissues. We performed PCRs using a universal primer set (27F and 1492R; Lane, 1991), the Promega Master Mix (Promega, Madison, WI, USA) and the following thermocycler conditions: initial denaturation at 94 °C for 4 min, 35 cycles of denaturation at 94 °C for 30 s, annealing (30 s) at 50 °C and elongation at 72 °C for 2 min, with a final elongation at 72 °C for 5 min. We then filtered all amplified products using Acro-Pro 100K-Omega filters (Pall Life Sciences, Port Washington, NY, USA), performed sequencing reactions using BigDye Terminator v3.1 Cycle Sequencing Ready Reaction Mix (Applied Biosystems, Foster City, CA, USA) and electrophoresed on an Applied Biosystems 3730 DNA Analyzer automated capillary sequencer running Sequencing Analysis v. 5.2 Software (Applied Biosystems).

We also sought to determine which form of the Calvin–Benson–Bassham enzyme RuBisCO was present in *Thyasira* cf. *gouldi* symbionts, as several magnetotactic bacteria had previously been shown to contain RuBisCO form II (*cbbM*) rather than form I (*cbbL*) (Bazylinski and Williams, 2006). To do so, we performed PCR with primer sets and conditions specific for RuBisCO forms I and II (Elsaied and Naganuma, 2001).

Molecular phylogenetic analysis and reconstruction

We used Sequencher (v. 5.2.3, Gene Codes, Ann Arbor, MI, USA) to edit the forward and reverse 16S sequences and used BLASTn (Altschul *et al.*, 1990) to identify the most closely related sequences in GenBank. We then aligned the consensus sequence with various other published sequences confirmed as magnetotactic bacteria or close relatives using Clustal W in MEGA5 (Tamura *et al.*, 2011). We constructed a phylogenetic tree using MrBayes (v. 3.2.2; Huelsenbeck and Ronquist, 2001) with GTR as the substitution model, rate variation set to gamma distribution with four discrete categories and allowance for invariant sites. Data sets were run twice, with initial settings of 10 000 000 generations each and a sampling frequency of once every 100 generations; however, once the convergence diagnostics hit the target value of 0.01, the analysis stopped resulting in a total of 442 trees read. The consensus tree was based on the 332 trees that were actually sampled. Support values at each node represent posterior probabilities calculated in MrBayes.

Detection of free-living symbionts in sediments

To determine whether free-living symbionts exist in sediments from the *Thyasira* cf. *gouldi* habitat, we first used fluorescence *in situ* hybridization (FISH) to label bacteria extracted from sediment samples, as in (Gros *et al.*, 2003). Based on the 16S rRNA sequence obtained, a 20-base oligonucleotide probe specific for *T.* cf. *gouldi* symbionts (5′-GCTCACC AAGGCAGCGATCC-3′, melting $T = 57.97$ °C) was designed using the Arb 5.5 probe design tool (Wolfgang *et al.*, 2004) and the gammaproteobacterial 16S rRNA Silva database as of 10 January 2013. Oligonucleotide probes were labeled with fluorescein at the 5' end. Although other sequences in GenBank were identical to the symbiont probe sequence, closest matches belonged to bacteria from terrestrial or hypersaline environments; therefore, the probe was considered to be specific to the *T.* cf. *gouldi* symbiont, at least within its native sediments (out of several possible probes, we selected the one that produced the least non-specific hits). To reduce the likelihood of unspecific binding, an unlabeled competitive probe with one-base difference (5′-GCT CACCAAGGCAACGATCC-3′, melting $T = 55.19$ °C) was used concurrently with the labeled probe in FISH assays (this approach was shown by Manz *et al.*, 1992 to drastically reduce non-specific binding). To test probe specificity and determine appropriate hybridization temperatures and formamide concentrations, symbionts extracted from a homogenized gill were filtered on a 0.22-μm black polycarbonate filter and hybridization was attempted under different conditions; binding was successful at 46 °C and with 40% formamide. Labeling with a fluorescein-labeled version of the competitive probe did not occur under these conditions.

Sediment cores (1 cm diameter) were collected from grab samples at the study sites, and subdivided into 0–2-, 2–5- and 5–10-cm-depth fractions. Samples were stored at −20 °C in equal volumes of fixative (4% formaldehyde in the following buffer: 40 g l^{-1} Borax in sterile 0.22 μm filtered seawater, pH 8.8), in 15-ml centrifuge tubes. Bacteria were

extracted from 1.5 ml of sediments by deflocculating using 250 μl of 100 mM sodium pyrophosphate and 3.25 ml of the above-mentioned buffer, followed by three cycles of sonication (10 s), and vortexing (30 s), and a final resting period of 15 min with periodic vortexing. Centrifuge tubes were then placed upright until most sediments appeared to have settled (1–3 min), and 1 ml of supernatant was filtered onto black 0.22 μm polycarbonate filters. Bacterial cells were permeabilized with 95% ethanol (1 min), placed on grease-covered slides and incubated with 50 ng probe in 38 μl hybridization buffer (40% formamide, 0.9 M NaCl, 20 mM Tris/HCl pH 7.4, 0.01% sodium dodecyl sulfate) at 46 °C for 2 h. Filters were then placed into 1.5 ml pre-warmed wash buffer (70 mM NaCl, 20 mM Tris/HCl pH 7.4, 5 mM EDTA, 0.01% sodium dodecyl sulfate) for 10 min, then rinsed with distilled water, dried and mounted on a slide using Permafluor for observation using a Zeiss Axio Imager A2 (Munich, Germany) with appropriate filter set. A sample of bacteria filtered from overlying seawater from the sampling site was used as a negative control; no fluorescent labeling occurred on these filters. Other filters containing sediment-extracted bacteria that had not gone through the hybridization process were tested for autofluorescence using the same filter set used for fluorescein detection; only very faint background fluorescence was noted on these filters.

Further confirmation of the presence of free-living forms of *Thyasira* cf. *gouldi* symbionts was obtained by searching for matching 16S sequence fragments among environmental DNA amplicons. Sediment samples from Deer Arm and Southeast Arm were collected in August 2013. Subsamples underwent total DNA extraction using the Xpedition Soil/Fecal DNA Miniprep kit (Zymo Research, Irvine, CA, USA) following the manufacturer's protocol for soil samples. PCR was then performed using barcoded (IonXpress, Life Technologies, South San Francisco, CA, USA) universal microbial primers targeting the hypervariable V6 region of the 16S rRNA gene developed by the Lang Lab of Memorial University, St. John's, NL, Canada (modified from Huber *et al.*, 2007). Reverse primers (5′-CGACRRCCATGCANCACCT-3′) contained the barcode while forward primers (an equal mix of: 5′-CTAACCGANGAACCTYACC-3′, 5′-ATACGCGARGAACCTTACC-3′, 5′-CNACGCGAAGAACCTTANC-3′ and 5′-CAACGCGMARAACCTTACC-3′) contained the Ion Torrent adapter sequences (for simplicity, the barcode and adapter sequences are not shown). PCRs were run using Phusion High Fidelity Polymerase and High Fidelity Buffer (New England Biolabs, Ipswich, MA, USA), and dNTPs used in standard concentrations. Thermocycler settings were as follows: 98 °C for 30 s, 30 cycles of 98 °C for 10 s, 72 °C for 30 s, followed by 72 °C for 2 min.

The PCR product was cleaned and prepared for sequencing on the Ion Torrent PGM (Life Technologies) following the protocol provided in the Ion PGM Template OT2 200 Kit and Ion PGM Sequencing 200 Kit v2. An Ion 314 v2 chip was used for sequencing. Runs were cleaned and filtered using the FastQC suite. Raw reads were trimmed at both ends to obtain a quality score >20. These were then aligned to the known 16S sequence of the *Thyasira* cf. *gouldi* symbiont as well as close relatives using the Torrent Mapping Alignment Program mapall command. Changes to the default settings included only the best alignments being accepted (-a 0) and an increase from the default 10% misalignment allowance to a 2% misalignment allowance (map1 –max-misalignment 0). The mapping results were then visualized using Integrative Genomics Viewer (Robinson *et al.*, 2011) and manually checked for misalignments.

Results

TEM and histology

Transmission electron micrographs of all symbiotic *Thyasira* cf. *gouldi* gills examined ($N>80$ individuals from various dates and from the three sampling sites) revealed numerous electron-dense octahedral inclusions within the cytoplasm of symbionts; in some cases, these inclusions formed the characteristic chains of magnetotactic bacteria (Figure 1a). In most sectioned bacteria, inclusions did not form a chain but were more or less aggregated in the bacterial cytoplasm (Figure 1b). Inclusions in chains measured 72.9 ± 28.8 nm ($N=20$ particles) and were more electron dense than inclusions not forming chains (55.7 ± 6.0 nm; $N=20$ particles).

Evidence of the endocytosis and digestion of symbionts by host cells (with the formation of characteristic whorls; Figure 1c) was visible in many gills. Symbiont inclusions resist host digestion and accumulate in whorls (size: 56.0 ± 6.3 nm; $N=20$ particles) and in host cytoplasm (size: 77.4 ± 11.1 nm; $N=20$ particles; Figure 1d). The abundance of bacterial inclusions varied widely among host specimens. Gill color was related to the overall abundance of inclusions, particularly in host cytoplasm: pink gills contained fewer inclusions than darker gills (based on general observations made on all the gills examined).

The cytoplasm of the bacteriocytes of five specimens (out of 11) stained intensely with prussian blue, revealing the presence of iron (Figure 2a). All specimens that were prussian blue positive had either dark or black gills.

Elemental analysis of inclusions

With ESEM, cellular structure could be observed in backscatter mode, and bacterial inclusions, sometimes forming chains, were visible (Figure 2b). X-ray spectra revealed the presence of iron in those structures (Figure 2c), but not in adjacent tissue.

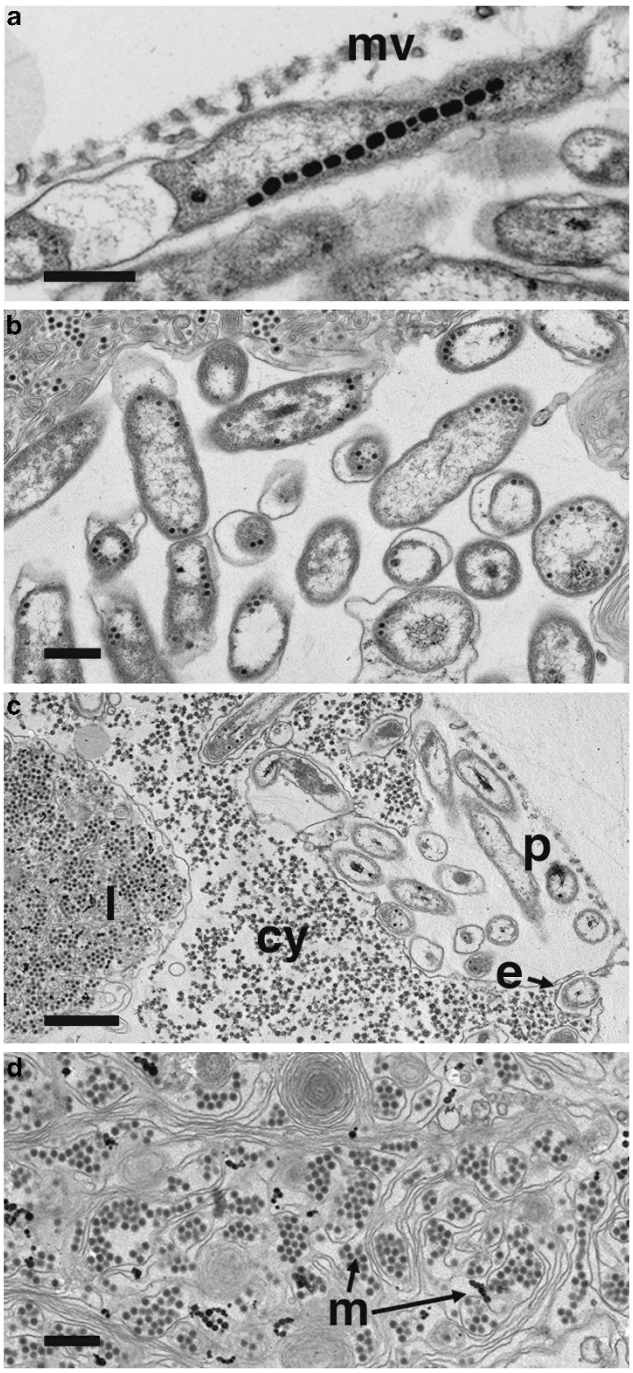

Figure 1 Transmission electron micrographs of symbionts associated with gill epithelial cells of *Thyasira* cf. *gouldi*. (**a**) Symbiont with a chain of magnetosomes, located close to the microvillar boundary (mv) of the bacteriocyte. Scale bar, 500 nm. (**b**) Multiple symbionts, with magnetosomes not organized in a chain. Scale bar, 500 nm. (**c**) View of symbionts in an extracellular 'pocket' (p), with some undergoing endocytosis (e). A large aggregate of lysed products of symbiont digestion (l), including magnetosomes, is visible in the host cytoplasm. Dark inclusions in the host cytoplasm (cy) may be the end products of lysosomal breakdown (that is, resistant particles of iron). Scale bar, 1 μm. (**d**) Magnified view of lysed bacterial whorls in the host cytoplasm; some magnetosomes appear in chains (m), others are in less dense aggregations. Scale bar, 500 nm.

Sulfur was also identified within the inclusions. Osmium in the sample was an artifact of the postfixation procedure.

Magnetic contrast in isolated symbionts

AFM topography images showed clumps of cellular material, with a height range of approximately 120 nm (Figure 3a), and MFM imaging revealed clear magnetic contrast in certain regions, measuring <200 nm (Figure 3b). The magnetic contrast remained evident at MFM tip fly heights of 100 nm, which is far beyond the distance over which van der Waals interactions would be significant.

Crystalline structure of inclusions

Five diffraction patterns were obtained using SAED, and the following d-spacings were determined: 2.94, 2.5 (two times), 1.56 (three times) and 1.8 Å. Comparisons with reference materials (greigite, magnetite, mackinawite, hematite and pyrite; Lennie *et al.*, 1995; Downs, 2006) indicate that inclusions are most likely a combination of greigite and mackinawite (Supplementary Table 1).

Symbiont identification and phylogeny

We amplified a single 16S rRNA sequence from each host specimen, with sequences from each host individual being exactly the same (length = 1430 bp, accession number: KJ658209), and used it to construct a phylogenetic tree (Figure 4). Symbionts belong to the gammaproteobacteria and are closely related to the symbionts of other invertebrates, including *Thyasira flexuosa* (98.5% identity, accession number L01575.1) and the hydrothermal vent tubeworm *Riftia pachyptila* (94% identity), as well as free-living bacteria from marine sediments (Figure 4). The magnetotactic bacterium that is most similar to the *T.* cf. *gouldi* symbiont (93% similarity) is gammaproteobacterium SS-5 isolated from the Salton Sea (Lefèvre *et al.*, 2012). Other more closely related bacteria are not known to have magnetosomes.

From the same DNA extracts, we amplified the gene for RuBisCO form II (*cbbM*, length = 397 bp, accession number: KJ658208), but could not amplify the gene for form I RuBisCO (*cbbL*). The most closely matched sequence (89% identity) was from a symbiont of a deep-sea tubeworm (*Lamellibranchia* sp., accession no. FM165442). There are no other thyasirid symbiont RuBisCO sequences available in GenBank.

FISH with the symbiont-specific 16S probe resulted in positive labeling of bacteria extracted from sediments collected at the three study sites, at all depth fractions examined. Following extraction of DNA from Bonne Bay sediments and analysis of PCR product sequences, we identified reads matching the known *Thyasira* cf. *gouldi* 16S sequence

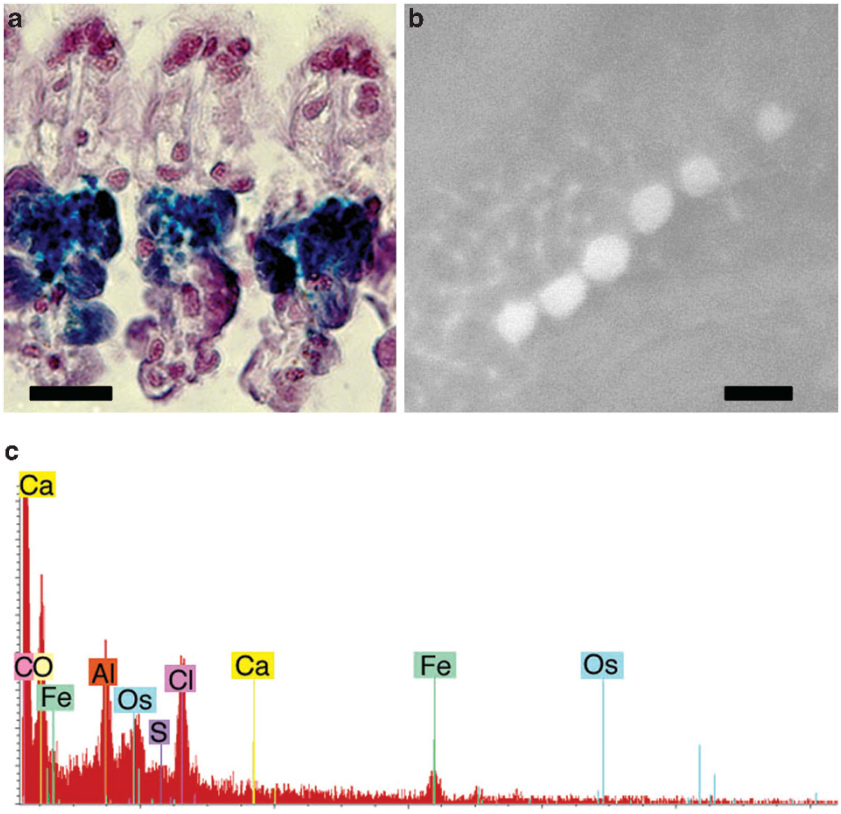

Figure 2 Iron determination in bacteriocytes and in the magnetosomes of *Thyasira* cf. *gouldi* symbionts. (**a**) Transverse section of a gill of *T.* cf. *gouldi*, stained with prussian blue and hematoxylin. The cytoplasm of bacteriocytes is intensely stained, indicating the presence of ferric iron. Scale bar, 20 μm. (**b**) Backscatter electron image of a symbiont, showing a chain of magnetosomes. Scale bar, 100 nm. (**c**) Energy dispersive X-ray spectrum after analysis of a particle within the magnetosome chain. Peaks for iron are visible.

with 98–100% similarity in both the samples. This level of specificity allows for natural mutations within the population as well as sequencing errors; other authors have considered that sequences >97% identical belong to the same microbial species (Huber *et al.*, 2007). Reads that aligned represented about 4% of the total data, suggesting that the symbiont represents a small portion of the bacterial community within these sediments. A blastn search revealed that the aligned reads were more similar to the *T.* cf. *gouldi* sequence than to any sequences available in the NCBI non-redundant database, with the top blast hits being 96% similar and originating from uncultured marine environmental samples. Therefore, there are free-living forms of the *T.* cf. *gouldi* symbionts in native sediments.

Discussion

Together, our results provide evidence for the presence of magnetosomes in the symbionts of *Thyasira* cf. *gouldi*, and allow us to propose a mechanistic pathway for symbiont acquisition in this species. We identified a single bacterial phylotype belonging to the sulfur-oxidizing gammaproteobacteria in *T.* cf. *gouldi*, as is typical of other thyasirids and many other chemosymbiotic bivalves (Dubilier *et al.*, 2008; Duperron *et al.*, 2012b). The single bacterial phylotype obtained from DNA extractions of *T.* cf. *gouldi* gills represents a symbiont and not simply an environmental contaminant trapped on epithelial cells, based on the following evidence: (1) numerous ($N>80$) symbiotic *T.* cf. *gouldi* specimens observed using TEM contain morphologically similar bacteria; (2) different host individuals ($N=3$ in this study) associate with the same, unique symbiont phylotype, a situation that would be highly unlikely if these bacteria were simply filtered from seawater; and (3) host epithelial cells clearly endocytose these bacteria similar to other bivalves where this process was demonstrated to be a pathway for nutrient transfer (Streams *et al.*, 1997).

TEM observations show that inclusions are common among *Thyasira* cf. *gouldi* symbionts and fall within the general range of morphologies and sizes (tens of nanometers) reported for magnetosomes (Lefèvre *et al.*, 2013a). The occasional chains of inclusions, along with the demonstration of iron (with magnetic properties) in both inclusions and host bacteriocytes show that those structures are not viruses, but rather magnetosomes. The diffraction patterns obtained from these inclusions suggest that particles are a mixture of the iron sulfides greigite

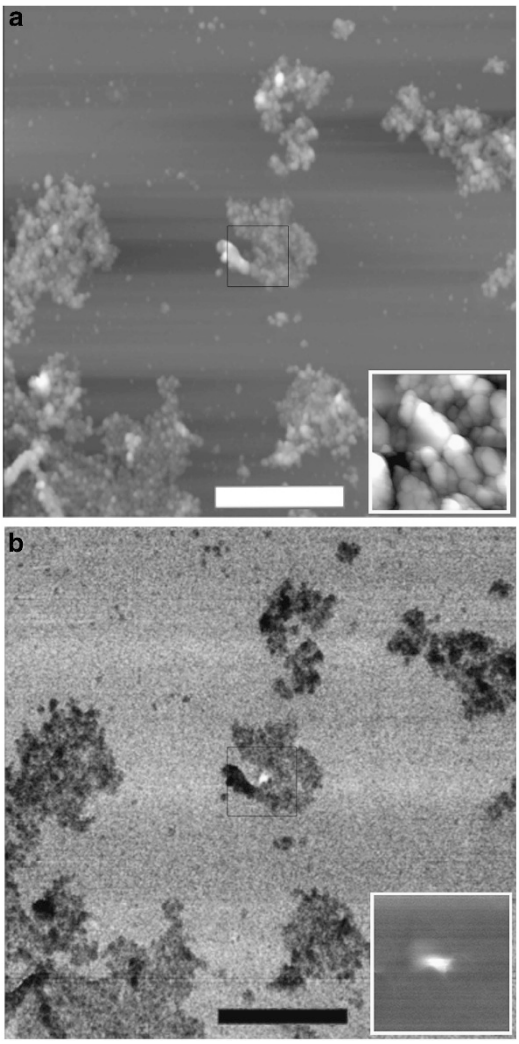

Figure 3 Simultaneously acquired AFM and MFM images of isolated *Thyasira* cf. *gouldi* symbionts. Scale bar, 5 μm. (**a**) AFM topography image of dried symbionts, where taller features are shown in white. Magnetosomes are not evident. Inset shows AFM image of outlined area. (**b**) MFM phase-contrast image of the area shown in **a** at a fly height of 100 nm. White and black regions indicate magnetic interactions between the sample and the magnetic tip. Inset shows MFM image of outlined area.

and its precursor mackinawite as in other marine and estuarine species of magnetotactic bacteria (Pósfai *et al.*, 1998), including gammaproteobacteria (Simmons *et al.*, 2004). Mackinawite is non magnetic and is converted to greigite in magnetotactic bacteria (this transformation was observed after sample preparation and exposure to air; Pósfai *et al.*, 1998), therefore, the presence of both forms of these minerals within a population of bacteria with magnetosomes is not surprising. The presence of those minerals is consistent with the identification of sulfur within inclusions using elemental analysis, and the shape of inclusions resembles that of other described greigite and mackinawite particles (Pósfai *et al.*, 1998; Spring and Bazylinski, 2006). Further, we noted less MFM signal than we expected in our bacterial cell preparations, which may indicate that an important fraction of the magnetosomes contained mackinawite in our preparations. Recently, a strain of sulfate-reducing magnetotactic deltaproteobacteria (BW-1) was shown to biomineralize both greigite and magnetite, depending on environmental conditions (Lefèvre *et al.*, 2011); another freshwater strain of deltaproteobacteria simultaneously produces magnetite and greigite (Wang *et al.*, 2013). We have no evidence for similar physiological capabilities in the symbiont of *T.* cf. *gouldi*, but given that only five diffraction patterns were obtained herein, we cannot affirm that this species is unable to biomineralize magnetite.

Although the presence of magnetotactic bacteria within a host organism appears counterintuitive as symbionts have no need for magnetotaxis, a consideration of the entire ecological spectrum of these bacteria, along with host behaviors, helps to elucidate their presence in host organisms. The existence of free-living symbionts in sediments from the *Thyasira* cf. *gouldi* habitat suggests horizontal symbiont transmission in these thyasirids. In their free-living state, the symbionts of *T.* cf. *gouldi* would benefit from magnetotaxis (or magneto-aerotaxis, Frankel *et al.*, 2006) as a means of tracking OAI in sediments, thereby facilitating sulfur oxidation for chemolithoautotrophy (as in other marine magnetotactic bacteria, Bazylinski and Williams, 2006). However, magnetotaxis would require the presence of flagella, which are not apparent on TEM images of gill-associated symbionts. The *T.* cf. *gouldi* symbiont is likely able to produce a flagellum when free living, and to lose it once associated with its host: the closely related, facultative symbiont of *Riftia pachyptila* (*Cad. Endoriftia persephone*) contains genes required for a functional flagellum and for chemotaxis, although flagella have never been observed in symbionts (Millikan *et al.*, 1999, Robidart *et al.*, 2008). Proteomic studies suggest physiological differences between host-associated and free-living states of *Cad. Endoriftia persephone* (Markert *et al.*, 2007), and physiological differences probably also exist between free living and associated *T.* cf. *gouldi* symbionts. In magnetotactic bacteria, the physiological state was shown to affect magnetosome formation (Bazylinski and Williams, 2006).

Thyasirid bioirrigation can produce OAI along burrow walls (Dando *et al.*, 2004; Hakonen *et al.*, 2010), thereby enhancing the concentration of magnetotactic bacteria in near-burrow sediments. *Thyasira* cf. *gouldi* could collect symbionts from burrow walls on the mucociliary surface of their elongated feet (Allen, 1958). Upon retraction of the foot within the mantle cavity, symbionts trapped in mucus could collect on the gill. Once associated with host cells, symbionts would have no requirement for a flagellum or a functional magnetosome, as the host acquires oxygen and sulfide through bioirrigation and sulfide-mining behaviors (Dufour

Figure 4 Bayesian phylogenetic tree constructed using 16S rRNA gene sequences (1627 positions in the alignment, see text for method used), showing the relationships between the *Thyasira* cf. *gouldi* symbiont, other gammaproteobacteria (symbiotic or free living) and known magnetotactic bacteria (in bold). Numbers represent posterior probabilities calculated in MrBayes (v. 3.2.2). Accession numbers are in parentheses.

and Felbeck, 2003; Dando *et al*., 2004). Interestingly, the biomagnetic crystals are rarely organized in a chain in *T*. cf. *gouldi* symbionts, suggesting that proteins responsible for chain formation are not maintained *in hospite*. Other magnetotactic bacteria with clusters of magnetosome crystals rather than chains retain magnetotactic abilities (Cox *et al*., 2002; Zhang *et al*., 2013); however, the crystals in those species are aggregated at one end of the bacterial cell and not scattered throughout the cytoplasm as in *T*. cf. *gouldi* symbionts. Further, the apparent presence of both mackinawite and greigite (with the former possibly predominating) in the gill-associated symbionts of *T*. cf. *gouldi* begs the question of whether mechanisms for transforming mackinawite to greigite remain functional in associated symbionts. The few *T*. cf. *gouldi* symbionts with intact chains of magnetosomes may be recently acquired individuals, suggesting that symbiont uptake in thyasirids can occur more than once in their adult life, as in lucinids (Gros *et al*., 2012).

The whorls in the bacteriocytes of *Thyasira* cf. *gouldi* indicate that host cells can engulf and digest symbionts, a likely means of nutrient uptake in thyasirids (Southward, 1986; Dufour, 2005). Through this process, magnetic particles appear resistant to host degradation, concentrating in whorls and in the cytoplasm of epithelial cells. However, particles within host cytoplasm are slightly larger and appear more diffuse than those within intact bacteria. Similarly, ciliates having engulfed magnetotactic bacteria accumulated enlarged magnetosomes in their cytoplasm (Martins *et al*., 2007), and the size increase was interpreted as showing magnetosome dissolution. Occasionally, host gills contain such dense concentrations of particles that they appear black; such gills stained intensely with prussian blue and were therefore iron-rich. *T*. cf. *gouldi* may eliminate magnetic particles through the renewal of epithelial cells, an active process in bivalve gills (Hanselmann *et al*., 2000).

Although much remains to be learned about the phylogeny and metabolic capabilities of *Thyasira* cf. *gouldi* (and other thyasirid) symbionts, 16S rRNA sequencing supports their phylogenetic placement among other sulfur-oxidizing gammaproteobacteria, and the amplification of type II RuBisCO provides evidence for autotrophic metabolism in these bacteria. The symbionts of *T*. cf. *gouldi* represent one of the few described magnetotactic gammaproteobacteria (Simmons *et al*., 2004; Lefèvre *et al*., 2012; Wang *et al*., 2013). Genomic studies have shown that

genes responsible for magnetosome formation are often organized within 'magnetosome islands' that contain mobile elements (Ullrich *et al.*, 2005; Jogler *et al.*, 2009), and recent work suggests a monophyletic origin for magnetotaxis within the proteobacteria (Lefèvre *et al.*, 2013b). Inclusions resembling magnetosomes, but interpreted as viruses, have been noted in other thyasirid symbionts, notably in 'symbiont of *Thyasira flexuosa* 1' from the Mediterranean, in Figure 4; (Brissac *et al.*, 2011), in symbionts of *T. gouldi* from Scotland (Southward and Southward, 1991) and of *T. flexuosa* from Long Beach, USA (Dufour, 2005) and Brest, France (J. Laurich, personal communication). Further phylogenetic and ecological studies of thyasirids and their symbionts should clarify why hosts from such different locations associate with closely related, magnetosome-forming symbionts.

The discovery of magnetotactic bacteria as symbionts of bivalves underscores their vast adaptability (Lefèvre and Bazylinski, 2013) and provides new opportunities to study magnetosome formation in an ecological context. The association of such bacteria with thyasirids is likely facilitated by the host's sulfide mining and bioirrigation activities, which produce OAI along burrow linings. In thyasirids, the combination of host and symbiont behaviors appears to have been key to chemosymbiosis establishment, enhancing the success of this family in a variety of sedimentary environments.

Conflict of Interest

The authors declare no conflict of interest.

Acknowledgements

R Hooper helped with specimen collection. M Shaffer, MUN Micro Analysis Facility, provided assistance with ESEM and A Korinek from the Canadian Centre for Electron Microscopy, McMaster University, performed SAED. H Fal and R Zadra assisted with histology and A Bullen performed RubisCO amplification. A Lang, Y Fu, H Munro, L Peña-Castillo helped with the analysis of environmental 16S sequences. Funding was obtained through NSERC Discovery Grant 386087-2010 (SCD), NSERC post-graduate scholarship (JRL), RDC Ignite R&D Grant 5404.1126.101 and RDC Ocean Industries Student Research Award (RTB).

References

Allen JA. (1958). On the basic form and adaptations to habitat in the Lucinacea (Eulamellibranchia). *Philos Trans Roy Soc B* **241**: 421–484.

Altschul SF, Gish W, Miller W, Myers EW, Lipman DJ. (1990). Basic local alignment search tool. *J Mol Biol* **215**: 403–410.

Batstone RT, Laurich JR, Salvo F, Dufour SC. (2014). Divergent chemosymbiosis-related characters in *Thyasira* cf. *gouldi* (Bivalvia: *Thyasiridae*). *PLoS ONE* **9**: e92856.

Bazylinski DA, Williams TJ. (2006). Ecophysiology of magnetotactic bacteria. *Microbiol Monogr* **3**: 37–75.

Brissac T, Rodrigues CF, Gros O, Duperron S. (2011). Characterization of bacterial symbioses in *Myrtea* sp. (Bivalvia: *Lucinidae*) and *Thyasira* sp. (Bivalvia: *Thyasiridae*) from a cold seep in the eastern Mediterranean. *Mar Ecol* **32**: 198–210.

Cox BL, Popa R, Bazylinski DA, Lanoil B, Douglas S, Belz A *et al.* (2002). Organization and elemental analysis of P-, S-, and Fe-rich inclusions in a population of freshwater magnetococci. *Geomicrobiol J* **19**: 387–406.

Dando PR, Spiro B. (1993). Varying nutritional dependence of the thyasirid bivalves *Thyasira sarsi* and *T. equalis* on chemoautotrophic symbiotic bacteria, demonstrated by isotope ratios of tissue carbon and shell carbonate. *Mar Ecol Prog Ser* **92**: 151–158.

Dando PR, Southward AJ, Southward EC. (2004). Rates of sediment suphide oxidation by the bivalve mollusc *Thyasira sarsi*. *Mar Ecol Prog Ser* **280**: 181–187.

Distel DL, Felbeck H. (1988). Pathways of inorganic carbon fixation in the endosymbiont-bearing lucinid clam *Lucinoma aequizonata*. part 1. purification and characterization of the endosymbiotic bacteria. *J Exp Zool* **247**: 1–10.

Downs RT. (2006). The RRUFF Project: an integrated study of the chemistry, crystallography, Raman and infrared spectroscopy of minerals. 19th General Meeting of the International Mineralogical Association, Kobe, Japan.

Dubilier N, Bergin C, Lott C. (2008). Symbiotic diversity in marine animals: the art of harnessing chemosynthesis. *Nat Rev Microbiol* **6**: 725–740.

Dufour SC. (2005). Gill anatomy and the evolution of symbiosis in the bivalve family *Thyasiridae*. *Biol Bull* **208**: 200–212.

Dufour SC, Felbeck H. (2003). Sulphide mining by the superextensile foot of symbiotic thyasirid bivalves. *Nature* **426**: 65–67.

Duperron S, Rodrigues CF, Léger N, Szafranski K, Decker C, Olu K *et al.* (2012a). Diversity of symbioses between chemosynthetic bacteria and metazoans at the Guiness cold seep site (Gulf of Guinea, West Africa). *Microbiologyopen* **1**: 467–480.

Duperron S, Gaudron SM, Rodrigues CF, Cunha MR, Decker C, Olu K. (2012b). An overview of chemosynthetic symbioses in bivalves from the North Atlantic and Mediterranean Sea. *Biogeosciences Discuss* **9**: 16815–16875.

Elsaied H, Naganuma T. (2001). Phylogenetic diversity of ribulose-1,5-bisphosphate carboxylase/oxygenase large-subunit genes from deep-sea microorganisms. *Appl Environ Microbiol* **67**: 1751–1765.

Frankel RB, Williams TJ, Bazylinski DA. (2006). Magnetoaerotaxis. *Microbiol Monogr* **3**: 1–24.

Gros O, Liberge M, Heddi A, Khatchadourian C, Felbeck H. (2003). Detection of the free-living forms of sulfide-oxidizing gill endosymbionts in the lucinid habitat (*Thalassia testudinum* environment). *Appl Environ Microbiol* **69**: 6264–6267.

Gros O, Elisabeth NH, Gustave SDD, Caro A, Dubilier N. (2012). Plasticity of symbiont acquisition throughout the life cycle of the shallow-water tropical lucinid *Codakia orbiculata* (*Mollusca*: Bivalvia). *Environ Microbiol* **14**: 1584–1595.

Hakonen A, Hulth S, Dufour S. (2010). Analytical performance during ratiometric long-term imaging of pH in bioturbated sediments. *Talanta* **81**: 1393–1401.

Hanselmann R, Smolowitz R, Gibson D. (2000). Identification of proliferating cells in hard clams. *Biol Bull* **199**: 199–200.

Huber JA, Welch DBM, Morrison HG, Huse SM, Neal PR, Butterfield DA *et al.* (2007). Microbial population structures in the deep marine biosphere. *Science* **381**: 97–100.

Huelsenbeck JP, Ronquist F. (2001). MRBAYES: Bayesian inference of phylogenetic trees. *Bioinformatics* **17**: 754–755.

Jogler C, Kube M, Schübbe S, Ullrich S, Teeling H, Bazylinski DA *et al.* (2009). Comparative analysis of magnetosome gene clusters in magnetotactic bacteria provides further evidence for horizontal gene transfer. *Environ Microbiol* **11**: 1267–1277.

Lane DJ. (1991). 16S/23S rRNA sequencing. In: Stackebrandt E, Goodfellow M (eds) *Nucleic Acid Techniques in Bacterial Systematics*. Wiley and Sons: New York, pp 115–175.

Lefèvre CT, Bazylinski DA. (2013). Ecology, diversity, and evolution of magnetotactic bacteria. *Microbiol Mol Biol Rev* **77**: 497–526.

Lefèvre CT, Menguy N, Abreu F, Lins U, Pósfai M, Prozorov T *et al.* (2011). A cultured greigite-producing magnetotactic bacterium in a novel group of sulfate-reducing bacteria. *Science* **334**: 1720–1723.

Lefèvre CT, Viloria N, Schmidt ML, Pósfai M, Frankel RB, Bazylinski DA. (2012). Novel magnetite-producing magnetotactic bacteria belonging to the Gammaproteobacteria. *ISME J* **6**: 440–450.

Lefèvre CT, Trubitsyn D, Abreu F, Kolinko S, Jogler C, Almeida LGP *et al.* (2013a). Comparative genomic analysis of magnetotactic bacteria from the Deltaproteobacteria provides new insights into magnetite and greigite magnetosome genes required for magnetotaxis. *Environ Microbiol* **15**: 2712–2735.

Lefèvre CT, Trubitsyn D, Abreu F, Kolinko S, Almeida LGP, Vasconcelos ATR *et al.* (2013b). Monophyletic origin of magnetotaxis and the first magnetosomes. *Environ Microbiol* **15**: 2267–2274.

Lennie AR, Redfern SAT, Schofield PF, Vaughan DJ. (1995). Synthesis and Rietveld crystal structure refinement of mackinawite, tetragonal FeS. *Mineral Mag* **59**: 677–683.

Manz W, Amman R, Ludwig W, Wagner M, Schleifer K-H. (1992). Phylogenetic oligodeoxynucleotide probes for the major subclasses of proteobacteria: problems and solutions. *Syst Appl Microbiol* **15**: 593–600.

Markert S, Ardnt C, Felbeck H, Becher D, Sievert SM, Hügler M *et al.* (2007). Physiological proteomics of the uncultured endosymbiont of *Riftia pachyptila*. *Science* **315**: 247–250.

Martins JL, Silveira TS, Abreu F, Silva KT, Silva-Neto ID, Lins U. (2007). Grazing protozoa and magnetosome dissolution in magnetotactic bacteria. *Environ Microbiol* **9**: 2775–2781.

Millikan DS, Felbeck H, Stein JS. (1999). Identification and characterization of a flagellin gene from the endosymbiont of the hydrothermal vent tubeworm *Riftia pachyptila*. *Appl Environ Microbiol* **65**: 3129–3133.

Pósfai M, Buseck PR, Bazylinski DA, Frankel RB. (1998). Iron sulfides from magnetotactic bacteria: structure, composition, and phase transitions. *Am Mineral* **83**: 1469–1481.

Proksch RB, Schäffer TE, Moskowitz BM, Dahlberg ED, Bazylinski DA, Frankel RB. (1995). Magnetic force microscopy of the submicron magnetic assembly in a magnetotactic bacterium. *Appl Phys Lett* **66**: 2582–2584.

Robidart JC, Bench SR, Feldman RA, Novoradovsky A, Podell SB, Gaasterland T *et al.* (2008). Metabolic versatility of the *Riftia pachyptila* endosymbiont revealed through metagenomics. *Environ Microbiol* **10**: 727–737.

Robinson JT, Thorvaldsdóttir H, Winckler W, Guttman M, Lander ES, Getz G *et al.* (2011). Integrative genomics viewer. *Nat Biotechnol* **29**: 24–26.

Sheehan DC, Hrapchak BB. (1980). *Theory and Practice of Histotechnology*, 2nd edition Mosby: St. Louis.

Simmons SL, Sievert SM, Frankel RB, Bazylinski DA, Edwards KJ. (2004). Spatiotemporal distribution of marine magnetotactic bacteria in a seasonally stratified coastal salt pond. *Appl Environ Microbiol* **70**: 6230–6239.

Spring S, Bazylinski DA. (2006). Magnetotactic bacteria. *Prokaryotes* **2**: 842–862.

Southward EC. (1986). Gill symbionts in thyasirids and other bivalve molluscs. *J Mar Biol Assoc UK* **66**: 889–914.

Southward EC, Southward AJ. (1991). Virus-like particles in bacteria symbiotic in bivalve gills. *J Mar Biol Ass UK* **71**: 37–45.

Streams ME, Fisher CR, Fiala-Médioni A. (1997). Methanotrophic symbiont location and fate of carbon incorporated from methane in a hydrocarbon seep mussel. *Mar Biol* **129**: 465–476.

Tamura K, Peterson D, Peterson N, Stecher G, Nei M, Kumar S. (2011). MEGA5: Molecular evolutionary genetics analysis using maximum likelihood, evolutionary distance, and maximum parsimony methods. *Mol Biol Evol* **28**: 2731–2739.

Ullrich S, Kube M, Schübbe S, Reinhardt R, Schüler D. (2005). A hypervariable 130-kilobase genomic region of *Magnetospirillum gryphiswaldense* comprises a magnetosome island which undergoes frequent rearrangements during stationary growth. *J Bacteriol* **187**: 7176–7184.

Wang Y, Lin W, Pan Y. (2013). High diversity of magnetotactic deltaproteobacteria in a freshwater niche. *Appl Environ Microbiol* **79**: 2813–2817.

Wolfgang L, Strunk O, Westram R, Richter L, Meier H, Yadhukumar AB *et al.* (2004). Arb: a software environment for sequence data. *Nucleic Acids Res* **32**: 1363–1371.

Zhang WY, Zhou K, Pan HM, Du HJ, Chen YR, Zhang R *et al.* (2013). Novel rod-shaped magnetotactic bacteria belonging to Alphaproteobacteria. *Appl Environ Microbiol* **79**: 3137–3140.

Supplementary Information accompanies this paper on The ISME Journal website (http://www.nature.com/ismej)